Description of *Zelonia daumondi* sp. nov. (Trypanosomatidae: Leishmaniinae)
Описание *Zelonia daumondi* sp. nov. (Trypanosomatidae: Leishmaniinae)

M.N. Malysheva, A.I. Ganyukova, D.O. Drachko, A.Y. Kostygov* & A.O. Frolov*
М.Н. Малышева, А.И. Ганюкова, Д.О. Драчко, А.Ю. Костыгов, А.О. Фролов

Marina N. Malysheva ⓘ, *Zoological Institute of the Russian Academy of Sciences, 1 Universitetskaya Emb., St Petersburg 199034, Russia. E-mail: malmarnik@yandex.ru*

Anna I. Ganyukova ⓘ, *Zoological Institute of the Russian Academy of Sciences, 1 Universitetskaya Emb., St Petersburg 199034, Russia. E-mail: anna.ganyukova@gmail.com*

Daria O. Drachko ⓘ, *Zoological Institute of the Russian Academy of Sciences, 1 Universitetskaya Emb., St Petersburg 199034, Russia. E-mail: sinderama@gmail.com*

Alexei Yu. Kostygov ⓘ, *Zoological Institute of the Russian Academy of Sciences, 1 Universitetskaya Emb., St Petersburg 199034, Russia. E-mail: kostygov@gmail.com*

Alexander O. Frolov ⓘ, *Zoological Institute of the Russian Academy of Sciences, 1 Universitetskaya Emb., St Petersburg 199034, Russia. E-mail: frolal@yandex.ru*

Abstract. Using light and electron microscopy, as well as molecular phylogenetic methods, we described a new species of monoxenous trypanosomatids, *Zelonia daumondi* **sp. nov.**, based on three isolates collected in northwestern Russia: two from the predatory pentatomid bug *Picromerus bidens* (Linnaeus, 1758) and one from an overwintering female mosquito *Culiseta annulata* (Schrank, 1776). This is the first record of a member of the genus *Zelonia* Shaw, Camargo et Teixeira, 2018 in the Holarctic Region and the most northern one in the world. All three studied isolates had identical sequences of the 18S rRNA and gGAPDH genes, justifying their assignment to a single species. An isolate previously documented in the lygaeid bug *Stalagmostethus fuscatus* (Turton, 1802) from Madagascar was found to belong to the same species, as determined by the 18S rRNA gene sequence, thereby demonstrating a wide geographic range of the new species.

Резюме. В данной работе, с использованием световой и электронной микроскопии, а также молекулярно-филогенетических методов, произведено описание нового вида моноксенных трипаносоматид *Zelonia daumondi* **sp. nov.** по трём изолятам, собранным на северо-западе России, а именно по двум – из хищного клопа-щитника *Picromerus bidens* (Linnaeus, 1758) и одному – из зимующей самки комара *Culiseta annulata* (Schrank, 1776). Это первая находка представителя рода *Zelonia* Shaw, Camargo et Teixeira, 2018 в Голарктике и самая северная в мире. Все три исследованных изолята имели сходную морфологию и идентичные последовательности генов 18S рРНК и gGAPDH genes и потому были отнесены к одному виду. Кроме того, один изолят, ранее обнаруженный у клопа-наземника *Stalagmostethus fuscatus* (Turton, 1802) с Мадагаскара, также относится к этому виду, судя по последовательности генов 18S рРНК, тем самым демонстрируя широкий ареал нового вида.

Key words: phylogeny, morphology, ultrastructure, *Picromerus bidens*, *Culiseta annulata*, new species

Ключевые слова: филогения, морфология, ультраструктура, *Picromerus bidens*, *Culiseta annulata*, новый вид

ZooBank Article LSID: 1211C84A-9330-4670-A365-7244FB142C8C

---

* Corresponding authors

Introduction

The number of genera of parasitic flagellates belonging to the family Trypanosomatidae has significantly increased in the last two decades (Kostygov et al., 2021). One of them is the genus *Zelonia* Shaw, Camargo et Teixeira, 2018 (subfamily Leishmaniinae), which was established to accommodate a species that had previously been described from the assassin bug *Ricolla simillima* Stål, 1859 (Reduviidae) in Costa Rica as *Leptomonas costaricensis* (Yurchenko, Lukes, Jirku, Zeledón et Maslov, 2006), based on typical promastigote organisation of cells (Yurchenko et al., 2006; Espinosa et al., 2018). The reason for the erection of the new genus was the phylogenetic position of this species, which proved to be distant from other *Leptomonas* spp. and more closely related to the dixenous members of the subfamily Leishmaniinae (i.e., *Leishmania* Ross, 1903, *Porcisia* Shaw, Camargo et Teixeira, 2018, and *Endotrypanum* Mesnil et Brimont, 1908), as well as endosymbiont-bearing *Novymonas* Kostygov et Yurchenko, 2020 and obscure *Borovskyia* Kostygov et Yurchenko, 2017 genera (Kostygov et al., 2016; Kostygov & Yurchenko, 2017; Espinosa et al., 2018).

Several other representatives of the genus *Zelonia* have been documented and/or described from various insects. The second species of the genus was described as *Z. australiensis* (nomen nudum)* based on a culture obtained from the blackfly *Simulium* (*Morops*) *dycei* Colbo, 1976 in Australia (Barratt et al., 2017). Three isolates closely related to *Zelonia costaricensis* (some of them apparently representing this same species) were detected in reduviids from Brazil and Panama (Espinosa et al., 2018). A strange trypanosomatid isolated from the mosquito *Haemagogus janthinomys* Dyar, 1921 in French Guyana was originally described as *Herpetomonas dedonderi* (Dedet, Geoffroy et Benichou, 1986) because of the presence of opisthomastigotes in the culture, although these co-existed with choanomastigotes, not typical for the species of *Herpetomonas* Kent, 1880 (Dedet et al., 2007). Recently, the inference of its phylogenetic position

using the 18S rRNA and gGAPDH genes justified placement of this species into the genus *Zelonia* (Boucinha et al., 2020). The previously unidentified isolates G755 obtained from a sandfly in Guatemala (Noyes et al., 1997) and COLPROT616 from the assassin bug *Rasahus surinamensis* Coscarón, 1983 were also found to be associated with *Zelonia*, as was a new isolate (M08) from the seed bug *Stalagmostethus fuscatus* (Turton, 1802) (Lygaeidae) (Boucinha et al., 2020; Votýpka et al., 2020). A total of three species of *Zelonia* have been described so far, and six additional isolates are known by their molecular sequences.

It was previously proposed that the geographic distribution of *Zelonia* species (either from the Southern Hemisphere or from Central America) could be explained by the predominant vicariance of these trypanosomatids since the existence of the Gondwana supercontinent. Moreover, this was also used as an argument in favour of the Gondwanan origin of dixenous Leishmaniinae (Barratt et al., 2017). Indeed, such a distribution is interesting and requires further analysis. However, it should also be noted that studies of the monoxenous trypanosomatid diversity have so far focused predominantly on tropical areas, while the Holarctic region has received much less attention in this regard.

Here we describe a new species of this poorly studied genus, *Zelonia daumondi* **sp. nov.**, based on three isolates from two different hosts: predatory shield bugs and mosquitoes collected in northwestern Russia. This is the first record of *Zelonia* in Russia and the Holarctic region in general, and, as such, it contradicts the view that the current geographical distribution of its species reflects the situation in past epochs and can be used for the reconstruction of the evolution of dixenous Leishmaniinae.

Material and methods

Dissection of insects and isolation of trypanosomatid cultures

Individuals of the spiny shield bug *Picromerus bidens* (Linnaeus, 1758) (Pentatomidae) were collected by A.O. Frolov in late August and early September of 2019 and 2020 in the Berezitsy Village of the Pskov Province (58°37′N, 28°54′E). Overwintering female mosquitoes *Culiseta annu-*

---

* The description was published in an electronic journal without being registered in the Official Register of Zoological Nomenclature (ZooBank), as required by the International Code of Zoological Nomenclature (articles 8.5.3 and 78.2.4).

lata (Schrank, 1776) (Culicidae) were collected by A.V. Razygraev on 30 October 2022 in three Sablino caves: Shtany, Grafskiy Grot and Pseudo-Santa-Maria (Tosno District, Leningrad Province, Russia; 59°40′N, 30°48′E) located close to each other (> 150 m).

The insects were euthanised in chloroform vapours and dissected in a drop of normal saline on a glass slide. The digestive system was examined by sections with a Leica DM 2500 light microscope, using differential interference contrast (DIC). The fragments of intestine containing trypanosomatids were placed into Schneider Drosophila Medium (Sigma-Aldrich, St Louis, USA) supplemented with 10% foetal bovine serum (BioloT, St Petersburg, Russia), 500 μg/ml of streptomycin, and 500 units/ml of penicillin (Sigma-Aldrich, St Louis, USA). After reaching a stable propagation of cultures, antibiotics were not used in subsequent passages. The purification of cultures from accompanying fungal contamination was performed using V-shaped tubes, as described earlier (Podlipaev & Frolov, 1987).

All obtained axenic cultures (isolates Pb7, Pb8 from *P. bidens* and M2604 from *C. annulata*) were cryopreserved and stored at -86 °C in the growth medium supplemented with 10% DMSO (Sigma-Aldrich, USA). They were deposited in the Research Collection of Parasitic Protists at the Zoological Institute of the Russian Academy of Sciences (St Petersburg, Russia).

Light microscopy, morphometry and statistical analysis

The smears prepared from the fragments of infected intestine and/or laboratory cultures were air-dried, fixed in 96% ethanol for 30 min, and then stained with Giemsa stain for 15–20 min at pH 6.8, or with 1 mg/ml 4′,6-diamidino-2-phenylindole (DAPI). Images were taken using the same microscope as above at ×1,000 magnification, with a UCMOS14000KPA 14-Mpx digital camera. Measurements of seven regular cell parameters (body length and width, nucleus length, free flagellum length, distance between nucleus and anterior end, distance between kinetoplast and anterior end, as well as the distance between nucleus and kinetoplast) were performed on the obtained images using ImageJ v. 1.53e software (Abramoff et al., 2004).

Comparison of cells of the same morphotype between isolates was performed using the Mann-Whitney test with Yates and Bonferroni corrections in R software v. 4.2.1 (R Core Team, 2022), while the differences between morphotypes in culture conditions were investigated using the principal component analysis (PCA) in PAST v. 4.0 software (Hammer et al., 2001). The raw data were used to create a correlation matrix, and two eigenvectors were extracted, providing two axes, onto which the raw data were projected to give a two-dimensional plot of the characters.

Electron microscopy

For transmission electron microscopy (TEM), precipitated cells of the five-day-old Pb7 culture were fixed with 1.5% glutaraldehyde in 0.1M cacodylate buffer for at least 1 h at 0 °C, post-fixed with 2% OsO4, dehydrated in an alcohol series followed by propylene oxide, and eventually embedded in an Epon-Araldite mixture. Ultrathin 60 nm sections were prepared using a UC-6 ultramicrotome, stained in a saturated aqueous solution of uranyl acetate and lead citrate following a previously described protocol (Reynolds, 1963). The sections were examined in a Morgagni 268-D electron microscope with an accelerating voltage of 80 kV.

For scanning electron microscopy (SEM), the suspension of cells was fixed and dehydrated as described previously (Ganyukova et al., 2019), placed on poly-L-lysine-coated slides, treated in a HCP-2 critical point dryer sputtered with a 20 nm platinum layer in an IB-5 ion coating device, and examined under a Tescan Mira3 LMU microscope at 25.00 kV.

DNA isolation, amplification and sequencing

Genomic DNA was isolated from intestinal fragments of infected insects and from cultures using the HiPure Blood DNA Mini Kit (Magen Biotechnology, China) according to the manufacturer's protocol. The nearly full-length (~2100 bp) trypanosomatid 18S rRNA gene was amplified from cultures with the commonly used primers S762 and S763 (Maslov et al., 1996). For intestinal samples, PCR was performed for a shorter (~850 bp) 18S rRNA gene fragment using the primers 1127F and 1958R (Kostygov & Frolov,

2007). The PCR fragments were sequenced using amplification primers and a set of internal primers as described before (Gerasimov et al., 2012). The gene for the glycosomal glyceraldehyde phosphate dehydrogenase gene (gGAPDH; ~1000 bp) was amplified using the primer pair M200-M201 as described previously (Maslov et al., 2010) and sequenced using the amplification primers. The obtained sequences were deposited in Gen-Bank under the following accession numbers: OR769954–OR769956 (18S rRNA gene) and OR757482–OR757484 (gGAPDH gene).

Phylogenetic analyses

The sequences of the SSU rRNA and gGAPDH genes obtained in this study were combined with those available in GenBank (electronic supplementary material, see the section "Addenda"). The alignment of sequences for both the SSU rRNA and gGAPDH genes was performed in MEGA v. 11 using the built-in MUSCLE module with default parameters (Kumar et al., 2018). For the gGAPDH gene, the sequences were dynamically translated to amino acids before alignment and reverse translated to nucleotides after it. The alignments of both genes were concatenated in MEGA, generating a dataset of 62 sequences with 3151 nucleotide positions.

Maximum likelihood tree reconstruction was performed in IQ-TREE v.1.6 (Nguyen et al., 2015) under the model GTR + F + R4 selected as the best by the built-in ModelFinder (Kalyaanamoorthy et al., 2017). Edge support was assessed using 1000 "standard" bootstrap replicates. Bayesian inference was performed in MrBayes v. 3.2.7 under the GTR + I + G4 model with 2,000,000 generations, and other parameters set by default (Ronquist et al., 2012).

Results

Prevalence of trypanosomatid infections and origin of laboratory cultures

We documented trypanosomatids in the gut of *Picromerus bidens* collected in the Pskov Province for two consecutive years. The infection prevalence was relatively high: ten out of twenty-five bugs (40%) in 2019 and one out of three (≈ 33%)

in 2020. Two axenic laboratory cultures, Pb7 and Pb8, were obtained from fragments of the infected intestine on the cultivation medium.

In the autumn of 2022, trypanosomatid infections were found in seven out of twenty-nine (24%) females of *Culiseta annulata* overwintering in caves. An axenic culture was obtained for the isolate M2604.

Phylogenetic analysis

The 18S rRNA gene sequences obtained in this work from bug hosts (both from the gut and from the cultures) were identical to each other as well as to that of *Zelonia* sp. M08 present in Gen-Bank is conspicuously distinct (97.3–99.2% identity) from the sequences of all described *Zelonia* species. The sequence of the isolate M2604 from the mosquito differed from the above by a single C/T transition. Thus, we concluded that the isolates studied here represent a new species, which we named *Z. daumondi* **sp. nov.** The sequences of the gGAPDH gene were also identical for all isolates of the new species except for M08, for which this comparison could not be done since the corresponding sequence is missing in GenBank.

The phylogenetic analyses confirmed the affiliation of the new species with the genus *Zelonia* (Fig. 1). More specifically, it formed a well-supported clade with *Z. costaricensis* and *Z. australiensis* Barratt, Kaufer et Ellis 2017. However, the exact relationships between the three species in this clade could not be reliably resolved (Fig. 1).

Light microscopy

In the intestine of *Picromerus bidens* (isolates Pb7 and Pb8), the trypanosomatids were represented by free-swimming promastigotes concentrated mostly in the midgut (Fig. 2A). They had long and thick flagella, the length of which often exceeded that of the cell body. The nucleus was round or oval and located in the first third of the cell. The kinetoplast was situated close to the anterior end of the cell, indicating that the flagellar pocket is rather shallow (Fig. 2A). In none of the intestinal sections, where the flagellates were present (from the foregut to the ileum), attached forms were detected. All measurements of the intestinal and cultural forms of flagellates are presented in Table 1.
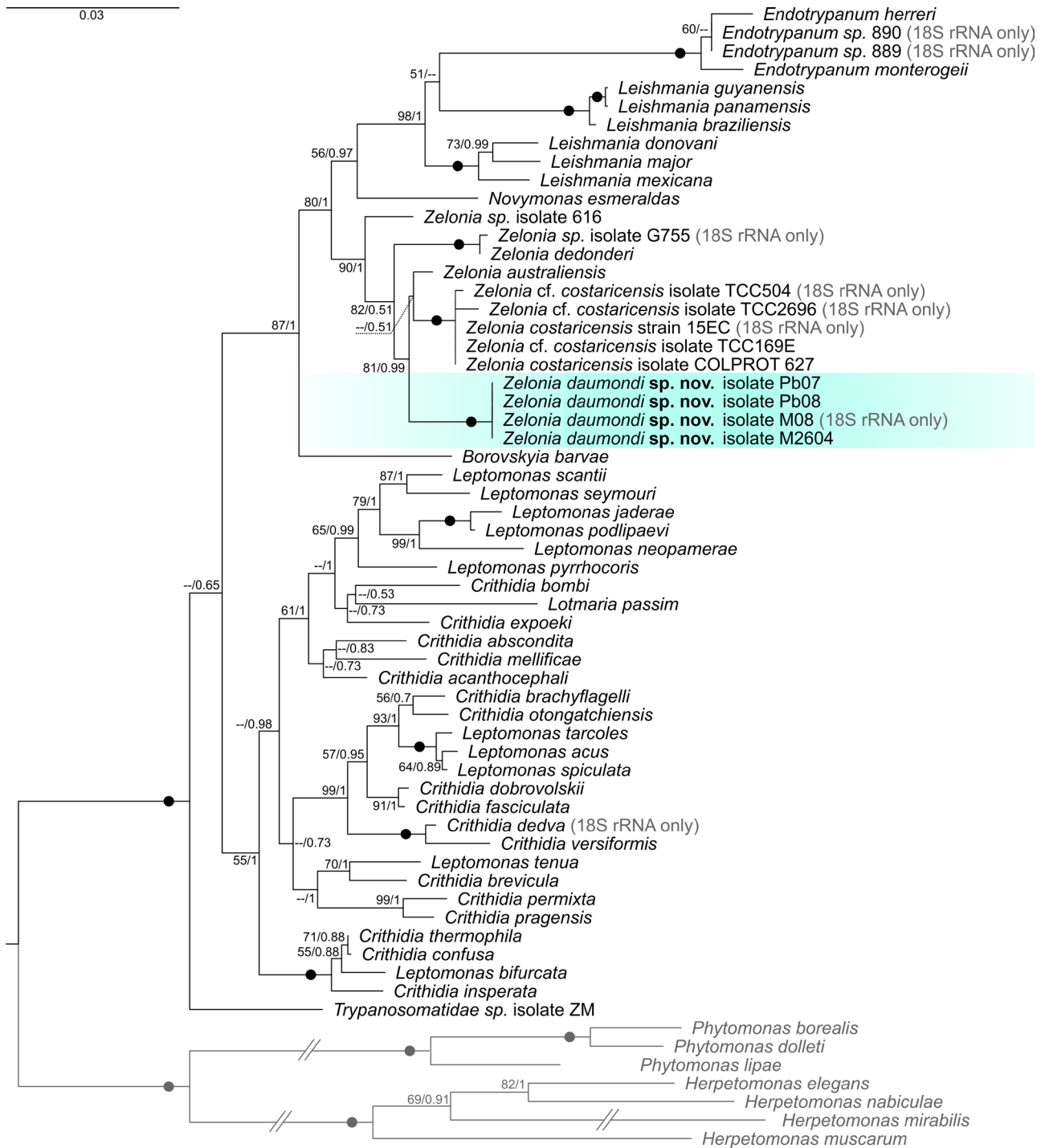
Fig. 1. Maximum likelihood phylogenetic tree of Leishmaniinae based on the concatenated sequences of the 18S rRNA and gGAPDH genes. Numbers at nodes represent bootstrap percentage and posterior probability, respectively. Values below 0.5 or 50% are replaced with double dashes; absolute supports by both methods are shown as black circles. Double-crossed branches are at 50% of their length. The tree is rooted with sequences of Herpetomonadinae (in grey). The position of the new species is highlighted in cyan. The scale bar denotes the number of substitutions per site.

Fig. 2. Morphology of the isolate Pb7. Light microscopy. **A**, in host (hapantotype), Giemsa staining, bright field; **B**, in culture, Giemsa staining, bright field; **C**, in culture, overlaid DIC and fluorescent microscopy, DAPI staining. Abbreviations: *f* – flagellum; *kp* – kinetoplast; *n* – nucleus; *op* – opisthomastigote; *par* – paramastigote; *pro* – promastigote. Scale bars: 10 μm.
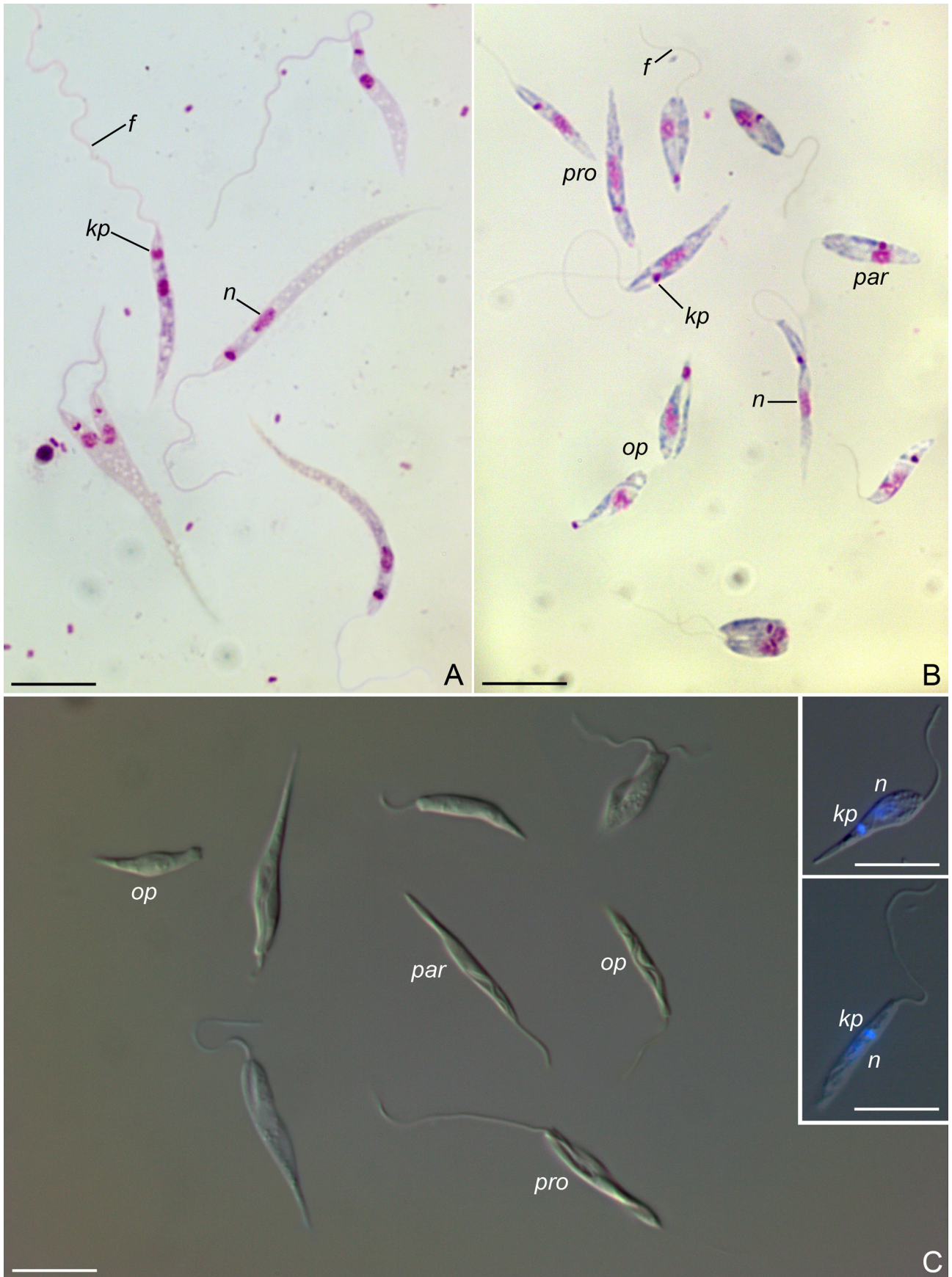
Table 1. Morphometry of trypanosomatid isolates from *Picromerus bidens* (Pb7) and *Culiseta annulata* (M2604). All measurements are in μm [median (min–max)].

Isolate & conditions	Length	Width	Flagellum	Nucleus	N–A	K–A	N–K
			Promastigotes				
Pb7 in the gut	31.2 (17.0–44.7)	1.6 (1.0–2.6)	33.8 (16.8–46.6)	3.2 (1.6–5.1)	8.0 (4.6–17.3)	2.4 (1.6–3.9)	4.8 (1.9–13.6)
Pb7 in the culture	17.6 (11.0–21.6)	1.9 (1.2–3.0)	19.4 (12.7–26.2)	3.1 (2.0–4.0)	5.3 (3.7–8.8)	3.0 (0.9–5.8)	1.7 (0.5–5.0)
M2604 in the culture	13.6 (9.3–22.5)	1.7 (0.6–2.5)	15.2 (11.0–21.4)	2.9 (2.1–3.9)	5.6 (4.0–10.2)	2.5 (1.7–5.0)	1.8 (0.8–7.5)
			Opisthomastigotes				
Pb7 in the culture	10.7 (8.4–13.9)	2.5 (1.9–3.8)	9.6 (3.7–18.4)	2.2 (1.5–3.0)	3.6 (1.7–5.2)	8.0 (5.6–10.7)	2.5 (0.8–8.2)
M2604 in the culture	8.4 (6.6–10.7)	2.2 (1.2–3.5)	9.0 (6.1–13.3)	2.5 (1.6–3.6)	3.6 (2.6–5.1)	5.9 (3.5–8.5)	0.3 (0.2–0.9)
			Paramastigotes				
Pb7 in the culture	11.2 (7.9–17.4)	2.6 (1.9–4.5)	13.8 (6.0–21.3)	2.4 (1.7–3.1)	4.5 (2.3–7.6)	5.9 (4.0–8.7)	0.4 (0.2–0.7)
M2604 in the culture	9.3 (7.4–12.2)	2.0 (1.3–2.9)	10.6 (6.8–14.1)	2.8 (1.9–3.7)	3.5 (2.5–7.1)	4.6 (2.5–6.7)	0.3 (0.1–0.6)

N–A, distance between nucleus and anterior end; K–A, between kinetoplast and anterior end; N–K, between nucleus and kinetoplast.

In *Culiseta annulata* (isolate M2604), the trypanosomatids occupied virtually the entire volume of the M2 midgut section (Fig. 3A). While the majority of them were free, those located in close proximity to the epithelium were attached. The detailed morphology of the intestinal forms for this isolate was not studied due to the low quality of the corresponding smear.

In the culture, *Zelonia daumondi* **sp. nov.** was represented by three morphotypes: in addition to promastigotes, there were also para- and opisthomastigotes (Figs 2B, C, and 3B). The promastigotes were considerably shorter (Table 1) than those in the gut, with a free flagellum sometimes longer than the cell body. The distance between the kinetoplast and the nucleus in these cells varied significantly (Table 1), indicating migration of the former, which should eventually lead to the transformation of the cell morphotypes. Comparison of the intestinal and cultural promastigotes of the isolate Pb7 using the Mann-Whitney test demonstrated that statistically significant differences (p < 0.002, n = 30–35) were also present in the flagellum length, distance between the nucleus and the anterior end of the cell, as well as that between the kinetoplast and the nucleus. At the same time, for most measurements, no significant differences (except for those in the length of flagellum with p = 0.003 and the cell body length with p < 0.02) could be observed between the Pb7 and M2604 cultures, isolated from different insect hosts.

The paramastigotes (cells with kinetoplast lateral to the nucleus) were shorter and wider than the promastigotes and had a proportionally shorter flagellum. Slight but statistically significant differences between these cells in the Pb7 and M2604 cultures were observed in all measurements, except for the length of the nucleus and its distances from the anterior end and the kinetoplast.

The opisthomastigotes were elongated, with the posterior end often pointed and the anterior one being conspicuously wider than in the promas-

Fig. 3. Morphology of the isolate M2604. **A**, in midgut of *Culiseta annulata* (DIC); **B**, in culture (bright field, Giemsa staining); **C**, in culture (SEM). Abbreviations: *f* – flagellum; *fp* – flagellar pocket; *kp* – kinetoplast; *n* – nucleus; *op* – opisthomastigote; *par* – paramastigote; *pro* – promastigote; white arrows – flagellar groove. Scale bars: 100 μm (A), 10 μm (B), 5 μm (C), 0.3 μm (inset).
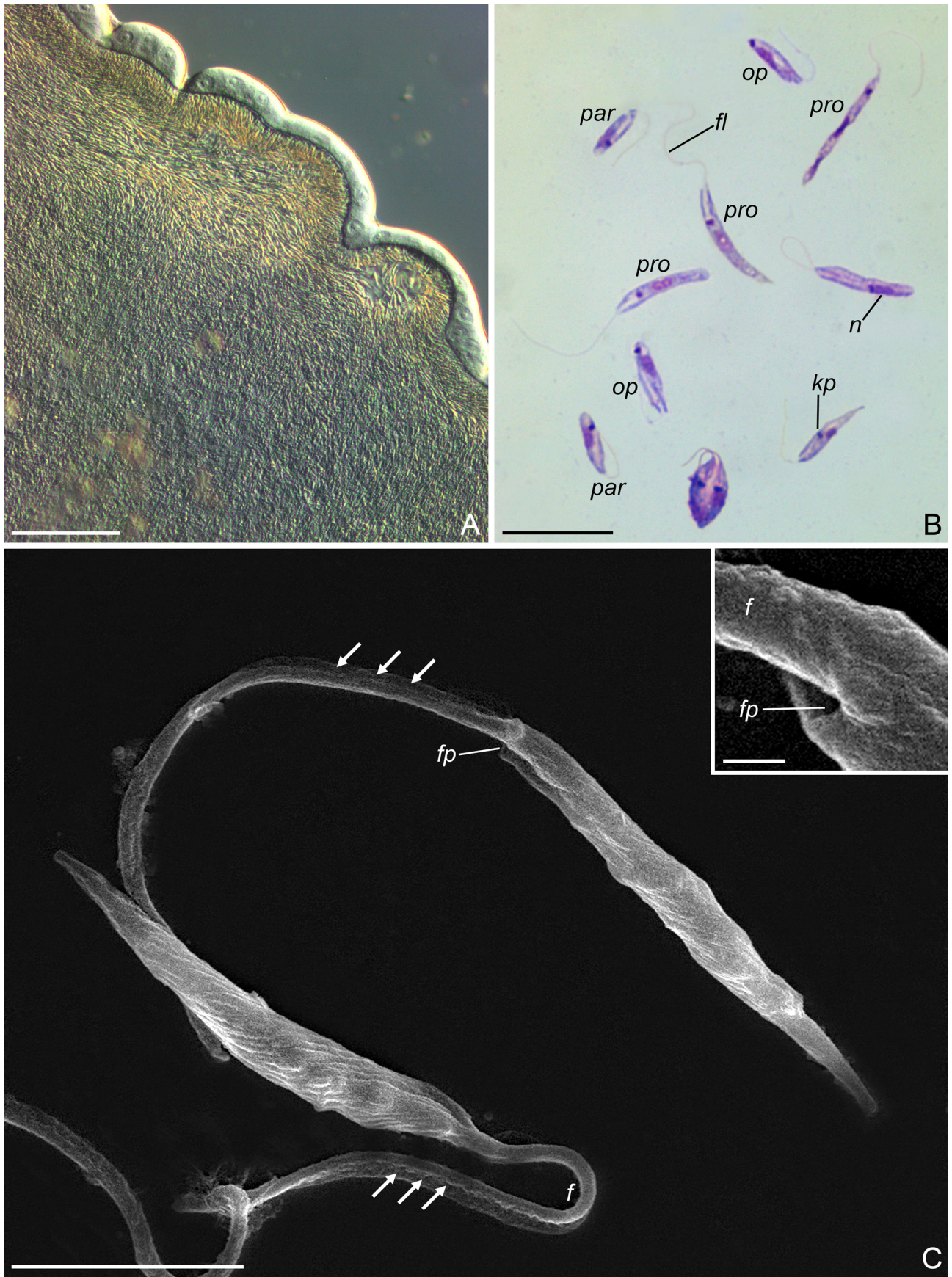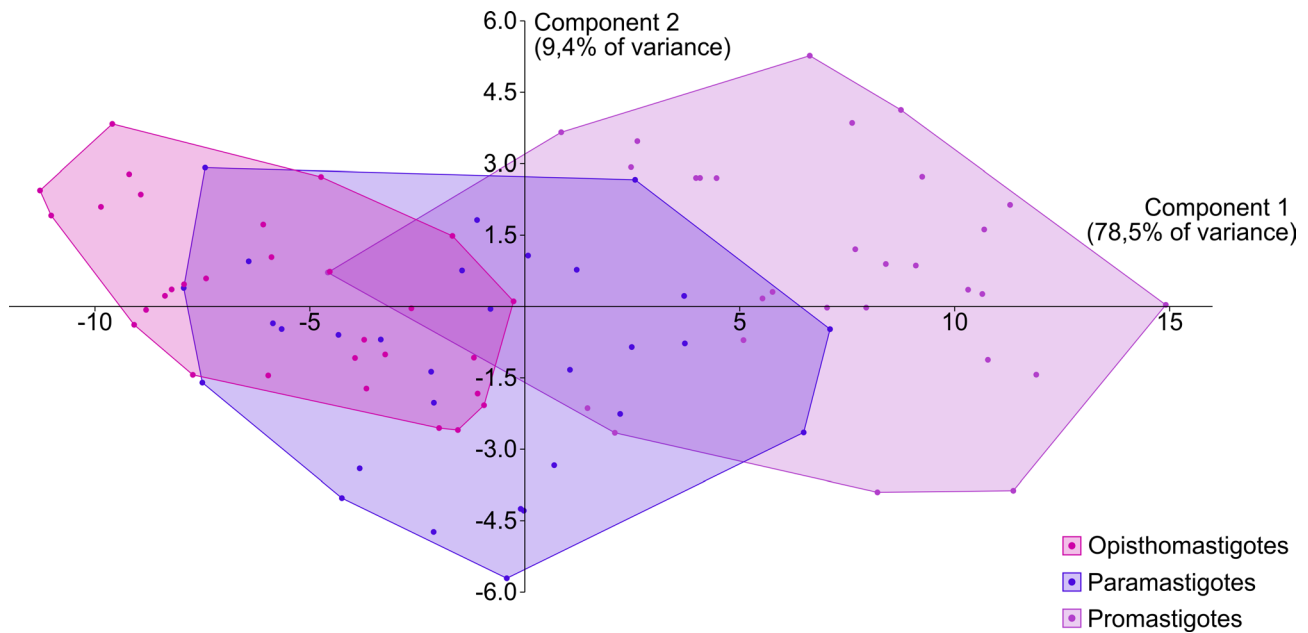
Fig. 4. PCA scatterplots for the three morphotypes observed in cell cultures (data combined from the Pb7 and M2604 isolates). Values in parentheses correspond to the proportion of variance for the components.

tigotes. The kinetoplast in these cells was usually in a terminal position. The free flagellum was comparable in length to the cell body. This morphotype demonstrated significant differences (with p-values ranging from 3.7×10^{-5} to 7.5×10^{-11}) in the cell length, distance of the kinetoplast from the anterior end, and that from the nucleus. The latter difference was especially pronounced (Table 1).

The DAPI staining of cells in the cultures did not reveal any other DNA-containing structures except for the nucleus and the kinetoplast (Fig. 2C – inset). This suggests the absence of endosymbiotic bacteria in the cultural forms.

The principal component analysis using the morphometric data demonstrated that the three above morphotypes have overlaps (Fig. 4). In the paramastigotes, most of the projection of the variance space overlapped with those in the pro- and opisthomastigotes. This is explainable by the fact that the paramastigotes represent intermediate forms between the two other morphotypes.

Electron microscopy

All three morphotypes had a standard set of organelles (nucleus, kinetoplast, mitochondrion, Golgi apparatus, glycosomes, and acidocalcisomes), generally organised as in other trypanosomatids (Fig. 5 A–C). Differences mainly concerned the position of the nucleus and the kinetoplast, as well as the depth of the flagellar pocket, which correlated with the latter (Fig. 5A–C). The kinetoplast DNA profile was long and narrow ($0.64-0.86 \times 0.09-0.13$ µm), with the length/width ratio varying from five to ten (Figs 5A, C, and 7A, C). Large multivesicular bodies (MVB) with mixed granular and vesicular contents have been observed in the posterior portion of the cells.

Fig. 5. Fine structure of different morphotypes, TEM. **A**, promastigote; **B**, opisthomastigote (inset, transverse section of flagellum); **C**, paramastigote. Abbreviations: *a* – axoneme; *ac* – acidocalcisome; *ag* – Golgi apparatus; *cv* – contractile vacuole; *f* – flagellum; *fp* – flagellar pocket; *gl* – glycosome; *kp* – kinetoplast; *mi* – mitochondrion; *mvb* – multivesicular bodies; *n* – nucleus; *pr* – paraflagellar rod; *sp* – spongiome; white arrowhead – flagellum attachment zone (FAZ); black arrowhead – groove of flagellum; black arrows – cytoplasmic microtubules. Scale bars: 1 µm (A–C), 0.3 µm (inset).
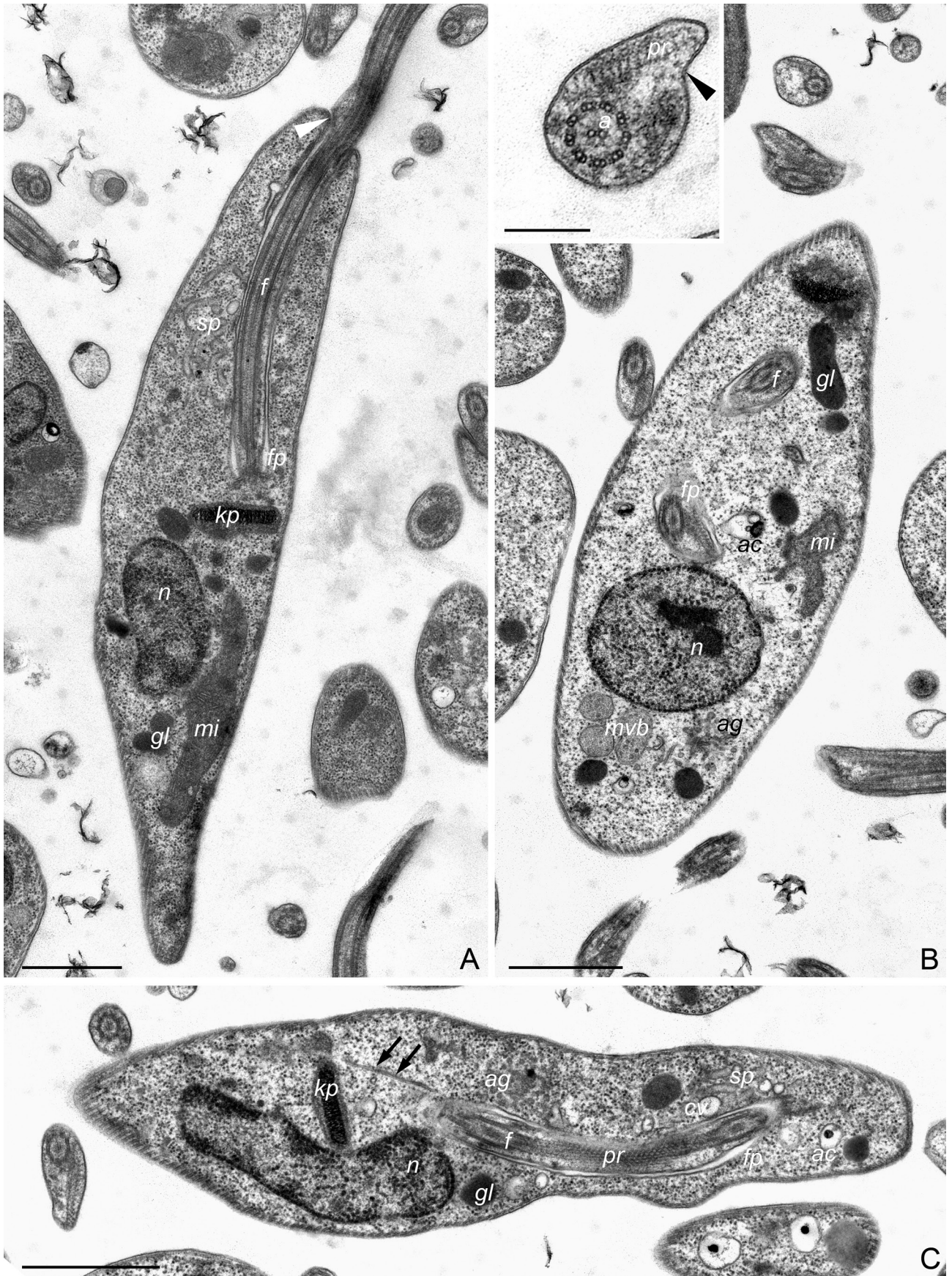
These membrane-bound structures tended to aggregate and seemed to be capable of budding (Fig. 5B). We believe that they are homologous to the organelles with the same name observed in trypanosomes and regarded as late endosomes, or, more broadly, part of the endosomal sorting complex involved in the process of intracellular vesicular transport (Silverman et al., 2013; Link et al., 2021).

The flagellar pocket passed eccentrically and, therefore, its lips were asymmetric: one of them was considerably wider and somewhat longer than another. This larger lip contained a well-developed spongiome with a contractile vacuole and, in its proximal part, also the Golgi apparatus (Figs 5A, C, 6A, and 7C). In some sections of this region, the glycosomes and acidocalcisomes could also be observed.

The flagellum formed a bulge right after the exit from the flagellar pocket. This bulge was ensured by the local distention of the flagellar matrix on the side opposite to the paraflagellar rod (PFR). In the proximal part of the bulge, there was a narrow area of contact between the flagellum and the large lip, known as the flagellar attachment zone (FAZ) (Fig. 6A, B). The contact between the pocket lip and the flagellum closed the entrance to the flagellar pocket from this side, while on the opposite one, there was a relatively small opening, which ensured the contact of the flagellar pocket with the environment (Fig. 3C – inset). The free flagellum was quite thick and had a conspicuous longitudinal groove across its length (Figs 3C and 5B – inset). The flagellum thickness was determined by the width of its PFR profile (400–600 nm), which exceeded the axoneme diameter by 2.0–2.5 fold. At the same time, the height of this profile was only 100 nm (Fig. 5B – inset). In the transverse sections of the flagellum, the PFR had a rod-like profile. Its proximal and distal domains were of the same thickness, being connected by the filaments of the intermediate domain oriented to the above at a 90° angle (Fig. 5B –inset).

In its narrow distal part, the flagellar pocket harboured a collar represented by a dense material underlaying the plasmalemma (Figs 6A, 7A). In the transverse sections, this collar had a horse-shoe-like profile (Fig. 6D). The flagellar pocket was armed with a microtubular quartet and two additional groups of microtubules: cytoplasmic and pocket ones. Two of these were arranged in a row perpendicular to the wall of the flagellar pocket (Fig. 6C, E) and apparently represented the cytoplasmic pair, as judged by the fact that only this pair was visible at the nucleus level, as well as by analogy with a previous study of *Leishmania mexicana* Biagi, 1953 (Wheeler et al., 2016). The cytoplasmic microtubules could be observed extending deep into the cytoplasm (Fig. 5C). The pocket group also consisted of two microtubules (data not shown), but in most sections only one of them was present (Fig. 6C). In agreement with the data on *L. mexicana* (Wheeler et al., 2016), the microtubular quartet and at least one of the two additional groups originated somewhere at the level of the flagellar pocket collar (Fig. 6D). Neither in the paramastigotes nor in the opisthomastigotes, the microtubular quartet was detected at the nucleus level, although the flagellar pocket extended into this area in both the morphotypes (Fig. 6E).

In the proximal part of the flagellar pocket, below the collar, exo- and endocytosis could be observed. Clathrin-coated vesicles formed on the walls of the flagellar pocket, thereby ensuring the transport of nutrients to the cell (Fig. 7A, B). End metabolites were excreted nearby in the form of exocytotic (= extracellular) vesicles (Fig. 7A–D). No traces of the cytostome-cytopharyngeal complex could be detected.

Discussion

The genus *Zelonia* is considered important from an evolutionary viewpoint, since it is the second closest (after *Novymonas*) relative of the

Fig. 6. Flagellum and flagellar pocket, TEM. **A**, longitudinal section; **B–E**, transverse sections at different levels. Abbreviations: *a* – axoneme; *ag* – Golgi apparatus; *cv* – contractile vacuole; *f* – flagellum; *faz* – flagellar attachment zone; *fp* – flagellar pocket; *fpc* – flagellar pocket collar; *gl* – glycosome; *mi* – mitochondrion; *mq* – microtubular quartet; *n* – nucleus; *pr* – paraflagellar rod; *sp* – spongiome; white arrows – pocket and cytoplasmic microtubules. Scale bars: 0.5 µm.
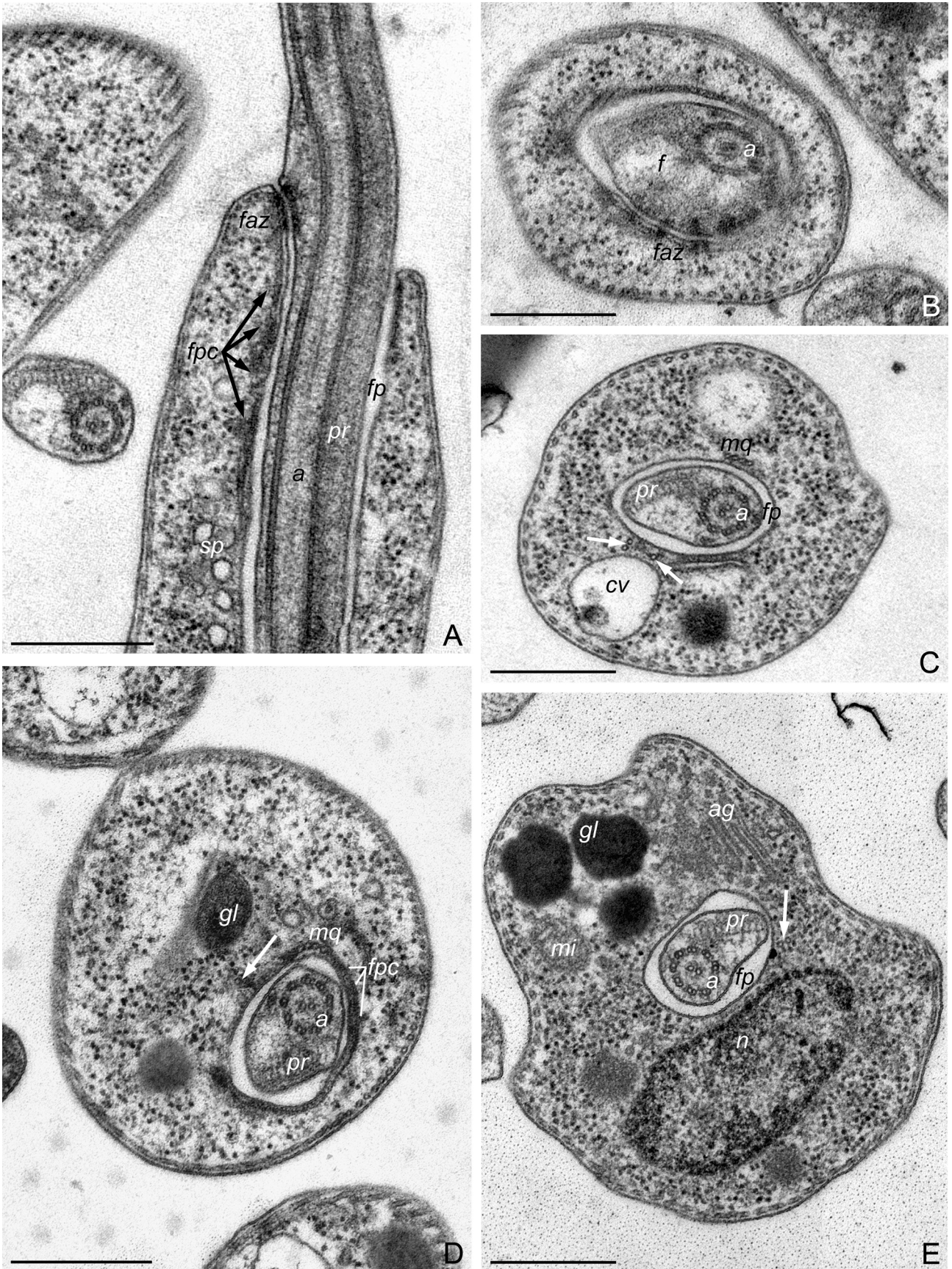
dixenous *Leishmania – Endotrypanum – Porcisia* clade (Kaufer et al., 2017; Kostygov et al., 2021). All species and undescribed isolates have been so far recorded only from the Neotropics, Madagascar, and Australia, which has been proposed as an argument in favour of the Gondwanan origin of the dixenous lifestyle in Leishmaniinae (Barratt et al., 2017; Kaufer et al., 2017; Votýpka et al., 2020). The isolates of the new species described here, *Zelonia daumondi* **sp. nov.**, represent the most northern record of *Zelonia*. However, as judged by the available sequence data, the isolate M08 (TU214) from the Madagascan lygaeid bug *Stalagmostethus fuscatus* (Votýpka et al., 2020) belongs to exactly the same species. Considering such a high dispersal potential within a species, the previous inferences based on the geographical distribution of *Zelonia* should be regarded as negligible.

Even with the relatively small number of records of all *Zelonia* species, some preliminary conclusions can be drawn with respect to their host distribution. From what can be seen now, the majority of the isolates originate from blood-sucking nematocerans or from predatory true bugs (Noyes et al., 1997; Yurchenko et al., 2006; Dedet et al., 2007; Barratt et al., 2017; Boucinha et al., 2020). The same picture has been observed for *Zelonia daumondi* **sp. nov.**, except for the additional record from the phytophagous true bug. Considering that the trypanosomatid diversity has been quite intensively screened in true bugs, but insufficiently in blood-sucking dipterans, we believe that only the latter represent specific hosts. Indeed, predatory bugs often become transitorily infected with trypanosomatids by consuming other insects; therefore, most of the records from such hosts are apparently non-specific (Králová et al., 2019; Frolov et al., 2021). As for the only phytophagous bug in the list of documented hosts, *Stalagmostethus fuscatus*, although the habits of this particular species have not been described in detail, it belongs to the family Lygaeidae, for which occasional predation and/or scavenging is supposed (Schaefer & Panizzi, 2000). In respect to the species described here, some additional arguments can be used. Firstly, the attachment of flagellates, as one of the indirect signs of a specific relationship, was observed only in the mosquito but not in the shield bugs. Secondly, *Picromerus bidens* overwinters in eggs, which cannot ensure the con-

tiguity of the parasite circulation, while *Culiseta annulata* outlives the cold season at the imaginal stage (and we detected the parasite exactly in an imago). Undoubtedly, to become conclusive, our view must be confirmed by studying details of the parasite developmental dynamics in experimental infections of the abovementioned hosts.

In the type species of the genus, *Zelonia costaricensis*, the promastigotes (more specifically, elongated, slightly flattened, and twisted ones) have been described as the only type of cells in culture (Yurchenko et al., 2006). However, in a later study, it was reported that the opisthomastigotes are present in the culture of the isolate TCC169, which belongs to the same species as judged by the 18S rRNA gene sequence (Espinosa et al., 2018). In the diagnosis of *Z. australiensis*, also only one morphotype has been mentioned, although with a notion about the high pleomorphism of promastigotes (Barratt et al., 2017). The most diverse cells have been reported in *Z. dedonderi*: pro-, para- and opisthomastigotes, both in the host and in the culture. However, promastigotes prevailed, and the proportion of the opisthomastigotes increased to 8–10% only after seven days of cultivation (Dedet et al., 2007). This is in line with our observation of *Z. daumondi* **sp. nov.**, where the opisthomastigotes become more abundant in older cultures. Thus, it appears that both the pro- and opisthomastigotes (as well as the intermediate stage, the paramastigotes) are characteristic of the genus *Zelonia*. It is currently unclear what the functional differences are between the morphotypes and what the differentiation triggers are. However, the higher proportion of opisthomastigotes in the old cultures suggests that this can be associated with a shortage of nutrients in the environment. It appears that in trypanosomatids, endo- and exocytosis occur exclusively in the flagellar pocket (Overath & Engstler, 2004; Field et al., 2007; Fernandes et al., 2020; Link et al., 2021), and since the latter in the opisthomastigotes has a bigger volume and surface, the transformation to this morphotype should increase the efficiency of the mentioned processes.

The study of the ultrastructure of the new species demonstrates its high similarity to *Z. costaricensis* in many respects, including the thick and long flagellum with a prominent PFR (with a characteristic rod-like profile) and a distinct groove
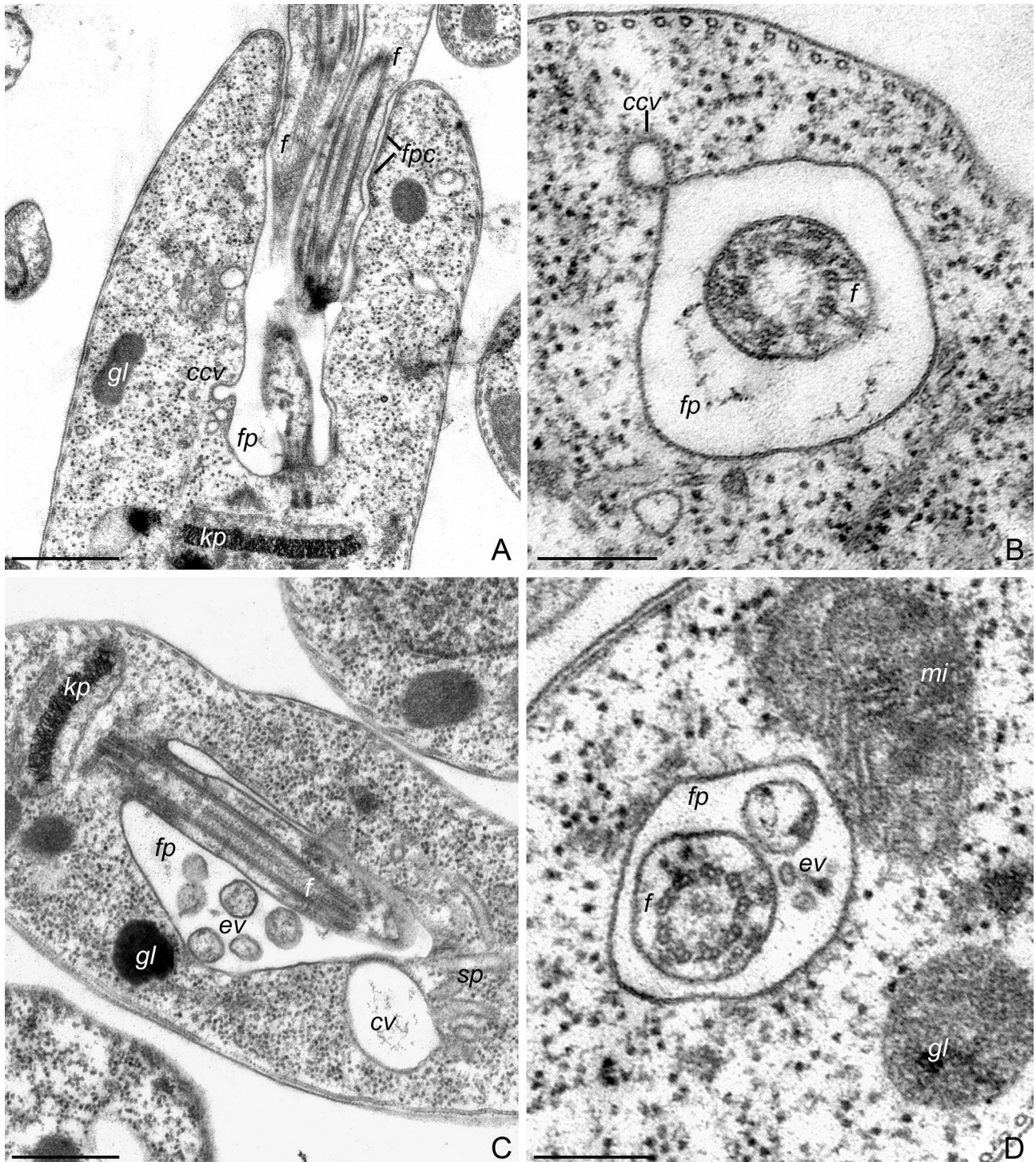
Fig. 7. Vesicular transport in the flagellar pocket, TEM. **A–B**, endocytosis; **C–D**, exocytosis. Abbreviations: *ccv* – clathrin-coated vesicles; *cv* – contractile vacuole; *ev* – exocytotic vesicles; *f* – flagellum; *fp*– flagellar pocket; *fpc* – flagellar pocket collar; *gl* – glycosome; *kp* – kinetoplast; *mi* – mitochondrion; *sp* – spongiome. Scale bars: 0.5 μm (A, C), 0.25 μm (B, D).

(Yurchenko et al., 2006). Regrettably, these details were not studied in all other *Zelonia* species. The asymmetry of the flagellar pocket described here has not been mentioned for the previously described species of the genus *Zelonia*. However, the published figures of all three previously described species allow observation of this feature, and those for *Z. dedonderi* also conspicuously demonstrate the presence of the FAZ on the terminal portion of the large lip of the pocket (Yurchenko et al., 2006; Dedet et al., 2007; Barratt et al., 2017). Most details of the flagellar pocket revealed here, including the collar, groups of supporting microtubules, and FAZ, are similar to those previously described in *Leishmania mexicana* (Wheeler et al., 2016), which agrees with their close phylogenetic relationship.

Taxonomic summary

Class **Kinetoplastea** Honigberg, 1963

Subclass **Metakinetoplastia** Vickerman, 2004

Order **Trypanosomatida** Kent, 1880

Family **Trypanosomatidae** Doflein, 1901

Subfamily **Leishmaniinae** Maslov et Lukeš, 2012

Genus *Zelonia* Shaw, Camargo et Teixeira, 2018

Zelonia daumondi Malysheva, Ganyukova et Frolov, **sp. nov.**
(Figs 2, 3, 5–7)

Hapantotype. Giemsa-stained slide Pb7–M2-hindgut and culture Pb7 deposited in the Research Collection of Parasitic Protists at the Zoological Institute of the Russian Academy of Sciences (St Petersburg, Russia).
Additional material. Smears Pb8 and M2604 and cultures Pb8 and M2604, the same collection as above.
Type locality. Berezitsy Village, Pskov Province, Russia.
Diagnosis. In host gut, cells represented by long promastigotes with flagella of comparable length. In culture, cells shorter and represented by three morphotypes: pro-, para- and opisthomastigotes. All cells with massive flagellum having broad paraflagellar rod and conspicuous longitudinal groove across its entire length. The species can be unambiguously distinguished from other species of the genus by the sequences of the 18S rRNA and gGAPDH genes (OR769954 and OR757482, respectively).

Comparison. *Zelonia daumondi* **sp. nov.** differs from *Z. costaricensis* (Yurchenko, Lukes, Jirku, Zeledón et Maslov, 2006) in the larger size of the promastigotes in culture (Barratt et al., 2017). From *Z. australiensis* (nomen nudum), it differs in the presence of the para- and opisthomastigotes (Barratt et al., 2017). From *Z. dedonderi* (Dedet, Geoffroy et Benichou, 1986), it differs in longer pro- and paramastigotes and their flagella, as well as shorter opisthomastigotes with longer flagella (Dedet et al., 2007). Considering that all these differences are based on the comparison of individual isolates and, moreover, were observed under cultivation in distinct nutritional media, they may be unreliable. Therefore, a clear distinction can be achieved only using the abovementioned gene sequences.

Hosts and localisation. *Picromerus bidens* (Linnaeus, 1758) (Heteroptera: Pentatomidae), all parts of intestine (type host); and *Culiseta annulata* (Schrank, 1776) (Diptera: Culicidae), midgut (M2).

Etymology. The new species is named after Dovmont, Prince of Pskov from 1266 to 1299; the specific name is derived from Daumondus, the Latin transcription of its name.

Addenda

Electronic supplementary material. GenBank accession numbers of sequences used in the phylogenetic analysis. File format: PDF. Available from: https://doi.org/10.31610/zsr/2023.32.2.252

Author contributions

A.I.G.: molecular analysis of isolates, scanning electron microscopy, statistical analysis, phylogenetic analysis; A.O.F.: collection and dissection of shield bugs, isolation of cultures; A.Yu.K.: analysis of sequences, writing and revising the manuscript; D.O.D.: molecular analysis of isolates; M.N.M.: dissection of mosquitoes, isolation of cultures, light microscopy, statistical analysis, transmission electron microscopy, writing the manuscript.

Acknowledgements

References

Abramoff M.D., Magalhaes P.J. & Ram S.J. 2004. Image processing with ImageJ. *Biophotonics Intern*, **11**(7): 36–42.

Barratt J., Kaufer A., Peters B., Craig D., Lawrence A., Roberts T., Lee R., McAuliffe G., Stark D. & Ellis J. 2017. Isolation of novel trypanosomatid, Zelonia australiensis sp. nov. (Kinetoplastida: Trypanosomatidae) provides support for a Gondwanan origin of dixenous parasitism in the Leishmaniinae. *PLOS Neglected tropical Diseases*, **11**(1): e0005215. https://doi.org/10.1371/journal.pntd.0005215

Boucinha C., Caetano A.R., Santos H.L., Helaers R., Vikkula M., Branquinha M.H., Dos Santos A.L.S., Grellier P., Morelli K.A. & d'Avila-Levy C.M. 2020. Analysing ambiguities in trypanosomatids taxonomy by barcoding. *Memorias do Instituto Oswaldo Cruz*, **115**: e200504. https://doi.org/10.1590/0074-02760200504

Dedet J.P., Geoffroy B. & Benichou J.C. 2007. Herpetomonas dedonderi n. sp. (Sarcomastigophora, Trypanosomatidae) from Haemagogus janthinomys Dyar, 1921 (Diptera, Culicidae). *Journal of Protozoology*, **33**(4): 530–533. https://doi.org/10.1111/j.1550-7408.1986.tb05657.x

Espinosa O.A., Serrano M.G., Camargo E.P., Teixeira M.M.G. & Shaw J.J. 2018. An appraisal of the taxonomy and nomenclature of trypanosomatids presently classified as Leishmania and Endotrypanum. *Parasitology*, **145**(4): 430–442. https://doi.org/10.1017/S0031182016002092

Fernandes A.C.S., Soares D.C., Neves R.F.C., Koeller C.M., Heise N., Adade C.M., Frases S., Meyer-Fernandes J.R., Saraiva E.M. & Souto-Padron T. 2020. Endocytosis and exocytosis in Leishmania amazonensis are modulated by bromoenol lactone. *Frontiers in cellular and infection Microbiology*, **10**: 39. https://doi.org/10.3389/fcimb.2020.00039

Field M.C., Natesan S.K., Gabernet-Castello C. & Koumandou V.L. 2007. Intracellular trafficking in the trypanosomatids. *Traffic*, **8**(6): 629–639. https://doi.org/10.1111/j.1600-0854.2007.00558.x

Frolov A.O., Kostygov A.Y. & Yurchenko V. 2021. Development of monoxenous trypanosomatids and phytomonads in insects. *Trends in Parasitology*, **37**(6): 538–551. https://doi.org/10.1016/j.pt.2021.02.004

Ganyukova A.I., Malysheva M.N., Smirnov P.A. & Frolov A.O. 2019. Crithidia dobrovolskii sp. n. (Kinetoplastida: Trypanosomatidae) from parasitoid fly Lypha dubia (Diptera: Tachinidae): morphology and phylogenetic position. *Protistology*, **13**(4): 206–214. https://doi.org/10.21685/1680-0826-2019-13-4-4

Gerasimov E.S., Kostygov A.Y., Yan S. & Kolesnikov A.A. 2012. From cryptogene to gene? ND8 editing domain reduction in insect trypanosomatids. *European Journal of Protistology*, **48**(3): 185–193. https://doi.org/10.1016/j.ejop.2011.09.002

Hammer Ø., Harper D.A.T. & Ryan P.D. 2001. PAST: Paleontological statistics software package for education and data analysis. *Palaeontologia electronica*, **4**(1): 9.

Kalyaanamoorthy S., Minh B.Q., Wong T.K.F., von Haeseler A. & Jermiin L.S. 2017. ModelFinder: fast model selection for accurate phylogenetic estimates. *Nature Methods*, **14**(6): 587–589. https://doi.org/10.1038/nmeth.4285

Kaufer A., Ellis J., Stark D. & Barratt J. 2017. The evolution of trypanosomatid taxonomy. *Parasites & Vectors*, **10**(1): 287. https://doi.org/10.1186/s13071-017-2204-7

Kostygov A.Y., Dobáková E., Grybchuk-Ieremenko A., Váhala D., Maslov D.A., Votýpka J., Lukeš J. & Yurchenko V. 2016. Novel trypanosomatid–bacterium association: evolution of endosymbiosis in action. *mBio*, **7**(2): e01985–01915. https://doi.org/10.1128/mBio.01985-15

Kostygov A.Y. & Frolov A.O. 2007. Leptomonas jaculum (Leger, 1902) Woodcock 1914: a leptomonas or a blastocrithidia? *Parazitologiya*, **41**(2): 126–136. (In Russian).

Kostygov A.Y., Karnkowska A., Votýpka J., Tashyreva D., Maciszewski K., Yurchenko V. & Lukeš J. 2021. Euglenozoa: taxonomy, diversity and ecology, symbioses and viruses. *Open Biology*, **11**(3): 200407. https://doi.org/10.1098/rsob.200407

Kostygov A.Y. & Yurchenko V. 2017. Revised classification of the subfamily Leishmaniinae (Trypanosomatidae). *Folia parasitologica*, **64**: 020. https://doi.org/10.14411/fp.2017.020

Králová J., Grybchuk-Ieremenko A., Votýpka J., Novotný V., Kment P., Lukeš J., Yurchenko V. & Kostygov A.Y. 2019. Insect trypanosomatids in Papua New Guinea: high endemism and diversity. *International Journal for Parasitology,*

49(13–14): 1075–1086. https://doi.org/10.1016/j.ijpara.2019.09.004

Kumar S., Stecher G., Li M., Knyaz C. & Tamura K. 2018. MEGA X: Molecular Evolutionary Genetics Analysis across computing platforms. *Molecular Biology and Evolution*, **35**(6): 1547–1549. https://doi.org/10.1093/molbev/msy096

Link F., Borges A.R., Jones N.G. & Engstler M. 2021. To the surface and back: exo- and endocytic pathways in Trypanosoma brucei. *Frontiers in cell and developmental Biology*, **9**: 720521. https://doi.org/10.3389/fcell.2021.720521

Maslov D.A., Lukeš J., Jirků M. & Simpson L. 1996. Phylogeny of trypanosomes as inferred from the small and large subunit rRNAs: implications for the evolution of parasitism in the trypanosomatid protozoa. *Molecular and biochemical Parasitology*, **75**(2): 197–205. https://doi.org/10.1016/0166-6851(95)02526-x

Maslov D.A., Yurchenko V.Y., Jirků M. & Lukeš J. 2010. Two new species of trypanosomatid parasites isolated from Heteroptera in Costa Rica. *Journal of eukaryotic Microbiology*, **57**(2): 177–188. https://doi.org/10.1111/j.1550-7408.2009.00464.x

Nguyen L.T., Schmidt H.A., von Haeseler A. & Minh B.Q. 2015. IQ-TREE: a fast and effective stochastic algorithm for estimating maximum-likelihood phylogenies. *Molecular Biology and Evolution*, **32**(1): 268–274. https://doi.org/10.1093/molbev/msu300

Noyes H.A., Arana B.A., Chance M.L. & Maingon R. 1997. The Leishmania hertigi (Kinetoplastida; Trypanosomatidae) complex and the lizard Leishmania: their classification and evidence for a neotropical origin of the Leishmania – Endotrypanum clade. *Journal of eukaryotic Microbiology*, **44**(5): 511–517. https://doi.org/10.1111/j.1550-7408.1997.tb05732.x

Overath P. & Engstler M. 2004. Endocytosis, membrane recycling and sorting of GPI-anchored proteins: Trypanosoma brucei as a model system. *Molecular Microbiology*, **53**(3): 735–744. https://doi.org/10.1111/j.1365-2958.2004.04224.x

Podlipaev S.A. & Frolov A.O. 1987. Description and laboratory cultivation of Blastocrithidia miridarum sp. n. (Mastigophora, Trypanosomatidae). *Parazitologiya*, **21**(4): 545–552. (In Russian).

R Core Team. 2022. *The R Project for Statistical Computing* [online]. Vienna: R Foundation for Statistical Computing. http://www.r-project.org/ [viewed 23 July 2022].

Reynolds E.S. 1963. The use of lead citrate at high pH as an electron-opaque stain in electron microscopy. *Journal of cell Biology*, **17**(1): 208–212. https://doi.org/10.1083/jcb.17.1.208

Ronquist F., Teslenko M., van der Mark P., Ayres D.L., Darling A., Hohna S., Larget B., Liu L., Suchard M.A. & Huelsenbeck J.P. 2012. MrBayes 3.2: efficient Bayesian phylogenetic inference and model choice across a large model space. *Systematic Biology*, **61**(3): 539–542. https://doi.org/10.1093/sysbio/sys029

Schaefer C.W. & Panizzi A.R. 2000. *Heteroptera of economic importance*. Boca Raton: CRC Press. 828 p.

Silverman J.S., Muratore K.A. & Bangs J.D. 2013. Characterization of the late endosomal ESCRT machinery in Trypanosoma brucei. *Traffic*, **14**(10): 1078–1090. https://doi.org/10.1111/tra.12094

Votýpka J., Kment P., Yurchenko V. & Lukeš J. 2020. Endangered monoxenous trypanosomatid parasites: a lesson from island biogeography. *Biodiversity and Conservation*, **29**(13): 3635–3667. https://doi.org/10.1007/s10531-020-02041-2

Wheeler R.J., Sunter J.D. & Gull K. 2016. Flagellar pocket restructuring through the Leishmania life cycle involves a discrete flagellum attachment zone. *Journal of cell Science*, **129**(4): 854–867. https://doi.org/10.1242/jcs.183152

Yurchenko V., Lukeš J., Jirků M., Zeledon R. & Maslov D.A. 2006. Leptomonas costaricensis sp. n. (Kinetoplastea: Trypanosomatidae), a member of the novel phylogenetic group of insect trypanosomatids closely related to the genus Leishmania. *Parasitology*, **133**(5): 537–546. https://doi.org/10.1017/S0031182006000746